

# MIMO Antenna Configuration for Femtocell Application

Landry Ndikumasabo

Roke Manor Research Ltd

Old Salisbury Lane

Romsey, SO51 0ZN

United Kingdom

landry.ndikumasabo@roke.co.uk

**Abstract**— Recent advances in the development of mobile applications have led to a need for mobile broadband platforms which support the capacity that these applications require. An investigation of possible antenna configurations that would be compatible with MIMO systems suitable for Femtocell applications is presented. A MIMO configuration of up to 6×2 antenna elements is modelled with the use of HFSS. Its performance is measured by means of the ideal-channel capacity increase it provides compared to a SISO architecture. The performance of the same MIMO configuration is then successfully modelled in Epsilon™ (Roke’s own channel modelling tool) with the use of a non-ideal indoor model. The simulations show that with the proposed configuration, it is possible to achieve a two-fold capacity increase compared to a SISO architecture in both channel conditions.

## I. INTRODUCTION

Various techniques such as High Speed Packet Access (HSPA) and Wideband Code Division Multiple Access (W-CDMA) have been developed to meet the stringent capacity requirements that modern mobile applications require. However, they still fall short of the required capacity as more bandwidth-intensive applications are being developed and as the mobile market embraces more internet-based services such as YouTube, iTunes and Skype.

The purpose of this project is to investigate possible antenna configurations that would be compatible with Multiple Input Multiple Output (MIMO) systems suitable for Femtocell applications. Such systems would lead to a capacity increase between the mobile phone and the Femtocell access point. The scope of this project is limited to the simulation of a suitable antenna configuration using spatial and pattern diversity techniques.

This paper starts by briefly explaining the relevant theory used in MIMO antenna development.

A Planar Inverted F Antenna (PIFA) element was chosen as the basis of the MIMO antenna configuration. It is modelled in HFSS and the resulting ideal-channel capacity is used as the performance metric.

The performance of the MIMO configuration modelled with HFSS is then evaluated with Epsilon™ in a non-ideal (indoor) environment made of concrete structures.

The performance of the configuration in both the ideal and non-ideal channels is analysed and conclusions are drawn.

## II. MIMO ANTENNA THEORY

This section explains the theory of a Multi-port Antenna (MPA) and includes modelling, mutual coupling, MIMO system network models and MIMO system performance measures.

### A. General Model of an MPA

The radiated field of an MPA can be expressed in terms of spherical waves, whose angular dependence is related to spherical modes (or harmonics), as shown in equation (1).

The normalised far-field radiation pattern  $F_i^A(\theta, \phi)$  due to the  $i^{th}$  input port of the MPA can be expressed in a modal expansion form as in [1] and [3]

$$F_i^A(\theta, \phi) = \sum_{j=1}^{\infty} S_{\beta\alpha_{ji}}^A \gamma_j(\theta, \phi) \quad (1)$$

where  $\gamma_j(\theta, \phi) \in C^{2 \times 1}$  forms a set of orthonormal spherical harmonic functions and  $S_{\beta\alpha_i}^A$  is the spherical mode expansion coefficients matrix as described in [2] and [6].

The scattering model of an MPA can then be expressed as [1]

$$\mathbf{b}^A = \begin{pmatrix} \mathbf{b}_{\alpha}^A \\ \mathbf{b}_{\beta}^A \end{pmatrix} = \begin{pmatrix} S_{\alpha\alpha}^A & S_{\alpha\beta}^A \\ S_{\beta\alpha}^A & S_{\beta\beta}^A \end{pmatrix} \begin{pmatrix} \mathbf{a}_{\alpha}^A \\ \mathbf{a}_{\beta}^A \end{pmatrix} = \mathbf{S}^A \mathbf{a}^A \quad (2)$$

where  $\mathbf{a}_{\alpha}^A \in C^{n \times 1}$  and  $\mathbf{b}_{\alpha}^A \in C^{n \times 1}$  are vectors describing the conventional, incident and reflected, scattering variables (conducted wave) at the input ports (the superscript, n, is the number of input ports) of the MPA.  $\mathbf{a}_{\beta}^A \in C^{\infty \times 1}$  and  $\mathbf{b}_{\beta}^A \in C^{\infty \times 1}$  are respectively, the infinite-dimensional column vectors representing the spherical mode expansion terms of the incoming and outgoing waves. The components  $S_{\alpha\beta}^A$  and  $S_{\beta\beta}^A$  describe the receiving and scattering properties of the MPA and  $S_{\alpha\alpha}^A$  describes the coupling and reflection coefficients between the input ports. The superscript  $A$  refers to either the transmit (T) or the receive (R) antennas; this notation applies for the rest of this paper. Note that  $\mathbf{S}^A$  is a matrix of matrices.

Assuming a perfect match between the antenna impedances and characteristic reference impedances at all the ports, the

elements of the MIMO channel matrix,  $\mathbf{H}$ , can be physically interpreted as [1]

$$h_{n,m} = \lambda \sum_{p=1}^P \left( \mathbf{F}_n^{R,p(\theta,\phi)} \right)^\dagger \mathbf{F}_{nm}^p \left( \mathbf{F}_m^{T,p(\theta,\phi)} \right) \quad (3)$$

where  $\lambda$  is the wavelength. For  $M$  transmitters and  $N$  receivers,  $p$  is the Multi-Path Component (MPC) between the  $m^{th}$  transmit and the  $n^{th}$  receive antennas.  $\mathbf{F}_m^T(\theta, \phi)$  and  $\mathbf{F}_n^R(\theta, \phi)$  are the normalised far-field transmit and receive radiation patterns and  $\mathbf{F}_{nm}^p$  is the polarimetric transfer matrix of the  $p^{th}$  MPC, which accounts for the gain, polarisation and phase between the  $m^{th}$  transmit (Tx) and  $n^{th}$  receive (Rx) antennas.  $\mathbf{F}_m^T(\theta, \phi)$  and  $\mathbf{F}_n^R(\theta, \phi)$  are available in a tabular format from HFSS simulations and are used to predict the channel,  $\mathbf{H}$ , with Epsilon<sup>TM</sup> (see Section III – B).  $\mathbf{F}_{nm}^p$  is related to the model representing the environment modelled with Epsilon<sup>TM</sup>.

Note that the channel referred to in (3) is the extended channel comprised of Tx, Rx and the actual propagation channel as described in [1].

## B. MIMO System Performance Measures

### 1) Antenna Correlation

The transmit covariance between the  $i^{th}$  and  $j^{th}$  antennas can be defined in terms of the transmit antenna characteristics as [1]

$$\mathbf{X}_{ij}^T = \int_{-\pi}^{\pi} \int_0^{\pi} \left( \frac{XPR}{1+XPR} \mathbf{F}_{i\theta}^T(\theta, \phi) \left( \mathbf{F}_{j\theta}^T(\theta, \phi) \right)^* \Psi_{\theta}^T(\theta, \phi) \right) \sin(\theta) d\theta d\phi \quad (4)$$

where  $\Psi_{\theta}^T(\theta, \phi)$  and  $\Psi_{\phi}^T(\theta, \phi)$  are the elevation and azimuth power spectrum at the transmitter, respectively and  $XPR$  is the cross-polarisation ratio, which is defined as the power ratio of the  $\theta$  and  $\phi$  components at the receiver.

The elements of the transmit antenna correlation matrix are then derived from (4) as

$$\mathbf{R}_{ij}^T = \frac{\mathbf{X}_{ij}^T}{\sqrt{\mathbf{X}_{ii}^T \mathbf{X}_{jj}^T}} \quad (5)$$

A similar approach can be followed for the receive side.

In an ideally scattered (isotropic) channel, it is assumed that the elevation and azimuth power spectra are uniform and that  $XPR$  equals to 1. It can then be shown that the covariance can be expressed in terms of the scattering characteristics at the input ports of the MPA only, as described in [1],

$$\mathbf{X}^A = \frac{1}{8\pi} (\mathbf{I} - \mathbf{S}_{\alpha\alpha}^A (\mathbf{S}_{\alpha\alpha}^A)^H) \quad (6)$$

where  $\mathbf{I}$  is the identity matrix and  $(\cdot)^H$  is the Hermitian operation. Hence  $\mathbf{X}^A$  is used to calculate  $\mathbf{R}_{ij}^T$  which is in turn used to calculate the value of  $\mathbf{H}$ , as shown in the next section.

### 2) MIMO System Capacity

Given an  $M \times N$  MIMO system, the general capacity expression, equivalent to the Shannon-Hartley equation (for a

transmitter without knowledge of the channel conditions), is [4]

$$C = \log_2 \det \left( \mathbf{I} + \frac{\rho}{M} \mathbf{H} \mathbf{H}^H \right) \quad (7)$$

where  $\rho$  is the average SNR at the transmitter.

For a number of channel realisations,  $Q$ , (7) can be transformed to the normalised ergodic capacity [1],

$$C_E = E \left\{ \log_2 \det \left( \mathbf{I} + \frac{\rho_0}{M} \mathbf{H}_0 \mathbf{H}_0^H \right) \right\} \quad (8)$$

where  $E\{\cdot\}$  denotes the mean or mathematical expectation of the  $Q$  capacities,  $\rho_0$  denotes the SNR at the receiver and  $\mathbf{H}_0$  denotes the normalised channel matrix.  $C_E$  is calculated via a Monte Carlo method by generating a number,  $Q$ , of random channel realisations. In this project, 10,000 channel realisations were used to calculate  $C_E$ . The  $q^{th}$  normalised channel is given by [1]

$$\mathbf{H}_0^q = \mathbf{H}^q \sqrt{\frac{N \times M \times Q}{\sum_{q=1}^Q \|\mathbf{H}^q\|_F^2}} \quad (9)$$

where  $\|\mathbf{H}^q\|_F^2$  is the square of the Frobenius norm given by [4]

$$\|\mathbf{H}^q\|_F^2 = \text{Trace}(\mathbf{H}^q \mathbf{H}^{qH}) \quad (10)$$

## C. MIMO Channel Model

The Kronecker model has been adopted as the model of choice because of its simple analytical manipulation. It has also been used in some IEEE standards such as IEEE 802.11n [5].

Given a non-line of sight propagation channel,  $\mathbf{H}$ , its Kronecker model is defined as

$$\mathbf{H} = (\mathbf{R}^R)^{\frac{1}{2}} \mathbf{W} \left( (\mathbf{R}^T)^{\frac{1}{2}} \right)^\dagger \quad (11)$$

$\mathbf{W} \in \mathcal{C}^{M \times N}$  is a complex random matrix with all elements being Independent Identically Distributed (IID) Gaussian random variables with zero-mean and unit variance and  $(\cdot)^\dagger$  is the transpose operation.  $\mathbf{R}^R \in \mathcal{C}^{N \times N}$  and  $\mathbf{R}^T \in \mathcal{C}^{M \times M}$  are the receive and transmit spatial correlation matrices, respectively.

The normalised Kronecker model for the  $q^{th}$  channel realisation is given by

$$\mathbf{H}_0^q = (\mathbf{R}_0^R)^{\frac{1}{2}} \mathbf{W}^q (\mathbf{R}_0^T)^{\frac{1}{2}} \quad (12)$$

The normalised transmit and receive correlation matrices are respectively given by

$$\mathbf{R}_0^T = \mathbf{R}^T \sqrt{\frac{N \times M \times Q}{\sum_{q=1}^Q \|\mathbf{H}^q\|_F^2}} \quad (13)$$

$$\mathbf{R}_0^R = \mathbf{R}^R \sqrt{\frac{N \times M \times Q}{\sum_{q=1}^Q \|\mathbf{H}^q\|_F^2}} \quad (14)$$

The normalisation is particularly useful because it allows the small changes in the channel, such as receive or transmit signal correlation, to be observed rather than being overshadowed by big changes, such as the path loss.

### III. ANTENNA CONFIGURATION

For the purpose of this project, a rectangular box measuring  $200 \text{ mm} \times 110 \text{ mm} \times 100 \text{ mm}$  (similar size to 800 Series Motorola Femtocell Access Point) was used and the operating frequency was chosen as 2 GHz ( $\lambda = 150 \text{ mm}$ ).

The configuration was initially developed using HFSS and evaluated in an ideal propagation channel. Its performance in a non-ideal propagation channel was predicted using Epsilon™. The resulting capacities for both the ideal and non-ideal channels were used as the performance metric. In order to calculate the capacity, the antenna characteristics at both ends of the communication link must be known. In this project, it is assumed that the Femtocell (the antenna configuration that is the subject of this project,  $M = 1, 2, \dots$ ) is on the transmitter side and that an arbitrary two element ( $N = 2$ ) antenna is on the receiver side. The SNR at the receiver was assumed to be 10 dB.

The scope of this paper is limited to the investigation of potential capacity increase resulting from spatial diversity. Future work will include polarisation diversity consideration.

#### A. HFSS Simulation

The quad-band PIFA antenna in Fig. 1 was used as the basis of the antenna configuration development.

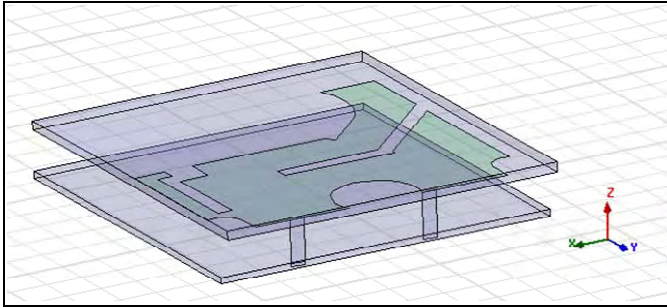


Fig. 1 PIFA antenna element used as the basis of the MIMO antenna configuration

With HFSS, the antenna configuration was gradually expanded from one element up to six elements (i.e. a single port antenna up to an MPA with six ports).

The final configuration comprised three antennas on the top side and three on the underside of the ground plane in a mirrored fashion as depicted in Fig. 2.

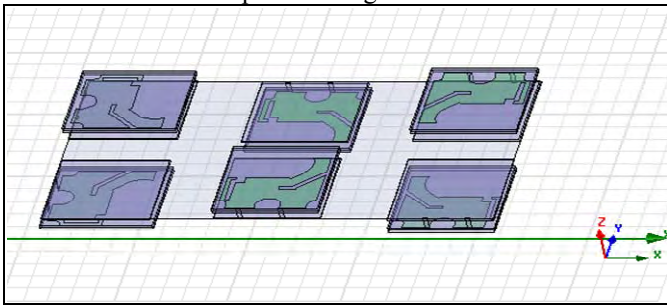


Fig. 2 The final MIMO Antenna configuration comprising of six elements

Recall that for an ideal channel, the S-parameter matrix at the input port of the antennas is sufficient to characterise the performance of the configuration. An S-parameter table

related to the configuration in Fig.2 was produced with HFSS. It was then used to calculate the correlation by combining (5) and (6).

Fig. 3 shows the resulting capacities, calculated by combining (8) and (12), as the number of antenna elements was gradually increased.

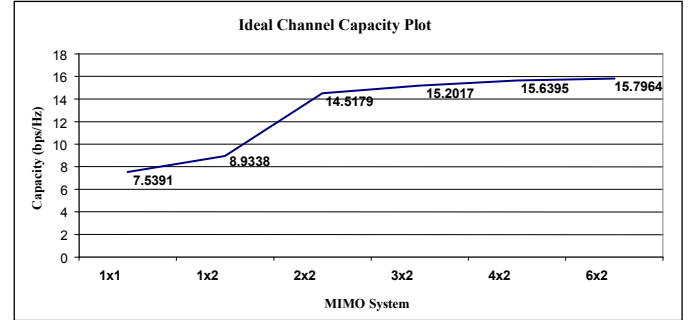


Fig. 3 Capacity increase Vs MIMO system

The increase in capacity is clearly observed. The saturation is explained by the fact that the data transmission modes, which allow for an increase in capacity, are limited by the minimum of  $M$  and  $N$ .

#### B. Epsilon™ Simulation

The performance of the 6-element configuration has shown that under ideal conditions, the capacity can be more than doubled for a MIMO configuration (up to  $6 \times 2$  MIMO in this case) compared to a Single Input Single Output (SISO) configuration.

This section describes the predicted performance of the same configuration as that modelled with HFSS under non-ideal conditions. Fig. 4 shows the indoor model that was used for the MIMO capacity predictions in Epsilon™. It also includes the positions of both the transmitter and receiver (connected by the solid line). In this case, the receiver moved along a corridor in five steps as shown in Fig. 4.

In order to facilitate the task, all the structures were set to ‘Concrete’ and were only reflective (no transmission through the walls) and the number of reflections was limited to five.

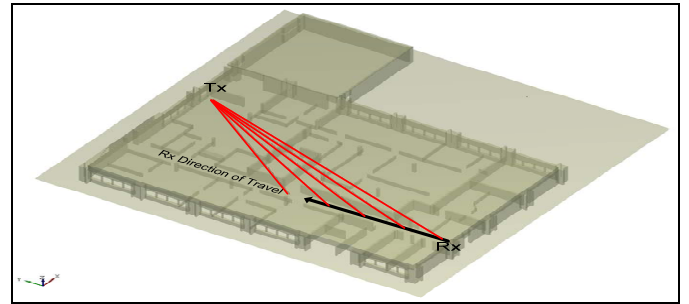


Fig. 4 Indoor model used to predict the performance of the MIMO antenna configuration with Epsilon™

Note also that in the case of non-ideal channel conditions, the radiation patterns of the antenna configuration are of primary importance in achieving a capacity increase. This can be explained by the definition of the channel elements predicted by Epsilon™, which is given by (4). Provided with the Tx and Rx radiation pattern tables and the environment model,

Epsilon<sup>TM</sup> directly predicts each element of  $\mathbf{H}$ , which is then used to calculate the capacity using (8), (9) and (10) with  $Q = 1$ . Care should therefore be taken in orientating the maximum gain in the correct direction.

The purpose of the Epsilon<sup>TM</sup> prediction is to model the MPA's performance in a non-ideal channel and highlight the performance difference in relation to the ideal channel.

The channel elements were obtained by individually predicting the MPC between  $Tx_m$  (for  $m = 1, 2, \dots, 6$ ) and  $Rx_n$  (for  $n = 1, 2$ ). Epsilon<sup>TM</sup> prediction results are a set of complex values representing the vertical, horizontal and cross-polar components, which can be used to calculate the capacity in both polarisations.

Table 1 presents the horizontal polarisation capacity calculation results (bps/Hz) obtained for all the configurations with the receiver travelling along the corridor in five equal steps.

TABLE I  
EPSILON<sup>TM</sup> PREDICTION CHANNEL CAPACITIES (BPS/Hz)

		Rx Positions				
		1	2	3	4	5
MIMO System	1x1	3.4594	3.4594	3.4594	3.4594	3.4594
	1x2	4.3923	4.3923	4.3923	4.3923	4.3923
	2x2	6.1183	4.4542	5.0613	4.4358	4.7279
	3x2	5.2477	4.4123	6.5098	5.7283	5.8619
	4x2	5.1472	4.4286	6.4582	5.8324	5.8124
	6x2	5.3497	4.4122	6.6945	5.8897	5.9313

A visualisation of Table 1 is provided in Fig. 5. Note that with Epsilon<sup>TM</sup>, it is possible to predict the performance of a MIMO system in an indoor environment (or outdoor) and produce a capacity map of the environment of interest. This could in turn be used to optimise system deployment.

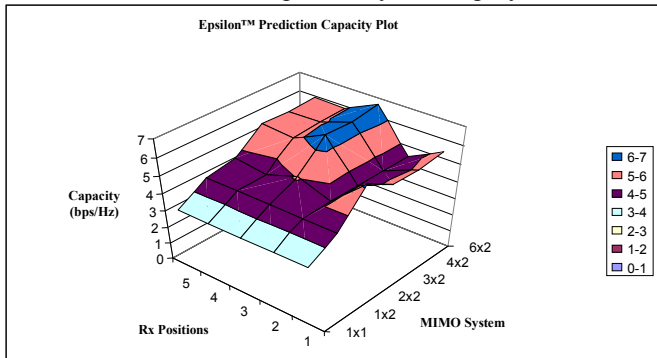


Fig. 5 Map of the predicted capacity in the indoor Epsilon<sup>TM</sup> model

The Epsilon<sup>TM</sup> prediction results show that there is an almost twofold increase in capacity moving from SISO to  $6 \times 2$  MIMO.

For comparison, Fig. 6 shows the Epsilon<sup>TM</sup> prediction results at Rx Position 3 plotted against the ideal channel results.

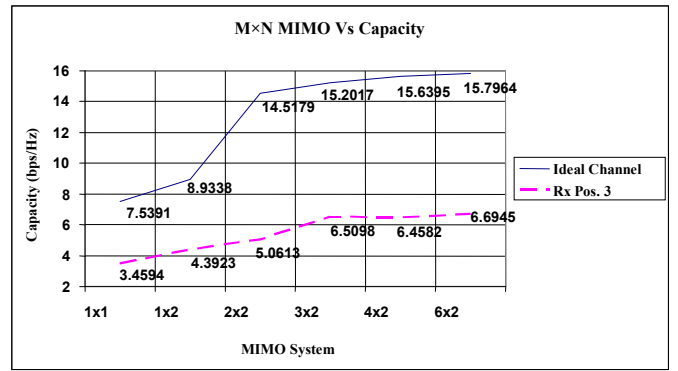


Fig. 6 Ideal Vs Non-ideal capacity plot

Notice the similarity in the equivalent capacity increase between the ideal and the non-ideal channels. The lower capacity level for the non-ideal channel is explained by the fact that the radiation patterns of the antennas used were not perfectly omni-directional and therefore some antenna gain might be directed away from the major MPC. It is therefore important to balance the trade-off between achieving low coupling (small S-Parameter values) and achieving an omni-directional radiation pattern (which low coupling could affect).

#### IV. CONCLUSION

The purpose of this project was to develop a MIMO antenna configuration suitable for the Femtocell application. A PIFA element was chosen as the basis of the configuration. Its performance was then measured in terms of the resulting capacity in an ideal channel (comprised of IID elements of zero-mean and unit variance). The performance of the same configuration was then predicted in Epsilon<sup>TM</sup> with a non-ideal (indoor) propagation channel.

The performance of the MIMO configuration in both the ideal and non-ideal channels achieved a capacity increase of about twice that of a SISO configuration.

#### ACKNOWLEDGEMENT

The author would like to thank Steve Simpson, Mike Jessup, Mary Mills and Kate Moore for their support.

#### REFERENCES

- [1] F. De Flaviis, L. Jofre, J. Romeu, A. Grau, "Multiantenna systems for MIMO Communications", Morgan & Claypool, 2008.
- [2] N. Marcuvitz, "Waveguide Handbook", Radiation Lab. Series, Vol. 10, McGraw Hill, 1951.
- [3] W. Wasylkiwskyj, "Response of an Antenna to Arbitrary Incident Fields", Antennas and Propagation Society International Symposium, IEEE 3B (2005), pp. 39 – 42, 2005.
- [4] A. Paulraj, R. Nabar, D. Gore, "Introduction to Space-Time Wireless Communication", Cambridge University Press, 2003.
- [5] "TGN Channel Models", IEEE Technical Report 802.11-03/940r4, Antennas and Propagation Society International Symposium, IEEE (2004).
- [6] Y. Chen, T. Simpson, "Radiation Pattern Analysis of Arbitrary Wire Antennas Using Spherical Mode Expansions with Vector Coefficients", IEEE Trans. Antennas and Propagation, Vol. 39, pp. 1716 – 1721, 1991.